ELECTRONIC SUPPLEMENTARY INFORMATION (ESI)

NMR relaxation and structural elucidation of peptides in the presence and absence of trifluoroethanol illuminates the critical molecular nature of integrin αvβ6 ligand specificity

Jane L. Wagstaff, Michelle L. Rowe, Shu-Ju Hsieh, Danielle DiCara, John F. Marshall,

Richard A. Williamson and Mark J. Howard

ESI CONTENTS

SUPPLEMENTARY MATERIALS AND METHODS

Details of Plasmid preparation and fusion protein expression and purification **2**

Detailed NMR data acquisition, processing and analysis for structure determination **3**

SUPPLEMENTARY RESULTS

Structure determination of peptides in 30%(v/v) trifluoroethanol **3**

Assignment of NMR spectra in the absence and presence of trifluoroethanol

Figure S1. *^{15}N HSQC spectra for peptides +/- TFE (with assignment labels)* **5**

Figure S2. *Structural ensembles with RMSD fits using the helix region* **6**

Additional ^{15}N relaxation figures

Figure S3. *^{15}N T_1, T_2 and hetNOE Relaxation data in the absence of TFE.* **7**

Figure S4. *^{15}N T_1, T_2 and hetNOE relaxation data in the presence of 30%(v/v) TFE* **7**

Figure S5. *^{15}N reduced spectral density data in the absence and presence of 30%(v/v) TFE* **8**

Figure S6. *Spectral density plots showing timescales of motion* **9**

FACS Data

Figure S7. *Binding of biotinylated peptides to A375P.puro and A375P.Beta6.puro by flow cytometry.* **10**

Additional Data

Figure S8. *^{15}N HSQC overlay of FMDV2 and reduced DBD1 peptide showing peptide similarities* **11**

Figure S9. *^{15}N HSQC overlay of LAP2 peptide and GST-fusion LAP peptide showing similarities* **12**

SUPPLEMENTARY TABLES

Table S1. *All peptide ^{15}N and ^{1}H NMR assignments in the absence and presence of 30%(v/v) TFE*

S-1.1 *Chemical shifts (ppm) of ^{15}N-DBD1 in PBS* **13**

S-1.2 *Chemical shifts (ppm) of ^{15}N-DBD1 in 30% d_3-TFE* **14**

S-1.3 *Chemical shifts (ppm) of ^{15}N-DBD2 in PBS* **15**

S-1.4 *Chemical shifts (ppm) of ^{15}N-DBD2 in 30% d_3-TFE* **16**

S-1.5 *Chemical shifts (ppm) of ^{15}N-A20fmdv2 in PBS* **17**

S-1.6 *Chemical shifts (ppm) of ^{15}NA20fmdv2 in 30% d_3-TFE* **18**

S-1.7 *Chemical shifts (ppm) of ^{15}N-A20lap2 in PBS* **19**

S-1.8 *Chemical shifts (ppm) of ^{15}N-A20lap2 in 30% d_3-TFE* **20**

Table S2. *Structural Statistics for the 50 ensemble structures of each peptide in 30% (v/v) TFE..* **22**

SUPPLEMENTARY REFERENCES **21**

SUPPLEMENTARY MATERIALS AND METHODS

Details of Plasmid preparation and fusion protein expression and purification

All laboratory reagents reagent grade or higher and supplied by Sigma-Aldrich unless otherwise stated. The production and purification of recombinant, isotopically enriched peptides was completed as previously described.[1] Briefly, sense and anti-sense oligonucleotides (MWG) were designed to encode peptide sequences: FMDV2 (NAVPNLRGDLQVLAQKVART), DBD1 (EKCPNLRGDLQVLAQKVCRT), DBD2 (CYVPNLRGDLQVLAQKVAKC), and LAP2 (GFFGRRGDLATIHGLNRPF). Oligonucleotides were 5' phosphorylated and designed with additional 3' overhangs of ATG for the sense and CAT for the anti-sense sequence so that annealed DNA could be ligated into the pET31b(+) (Novagen) vector pre-cut with A*lw*N I restriction enzyme. Oligonuclotides were inserted downstream of the N-terminal fusion protein ketosteroid isomerase and upstream of a C-terminal His-tag. Ligation mixtures were transformed into competent *E. coli* DH5α cells and selected for by plating on ampicillin LB agar plates. Colonies were screened for oligonucleotide insertion by PCR or restriction digestion of purified plasmid using *Xba* I and *Xho* I restriction enzymes. Sequences of plasmids containing multiple inserts were sequenced and if correct transformed into competent *E. coli* BL21(DE3) cells ready for recombinant protein expression.

Recombinant ^{15}N isotopically enriched fusion protein was expressed in minimal M9 medium at 37 °C at 200 rpm with ^{15}N ammonium sulphate (Cambridge Isotopes, USA) as the sole nitrogen source. Protein expression was induced by addition of IPTG to a final concentration of 1 mM for 3-4 h when the OD_{600nm} of the culture was between 0.55 and 0.7. Cells were harvested by centrifugation (15 min, 6300 g) and the cell pellet re-suspended in lysis buffer (20 mM NaH_2PO_4, 50 mM NaCl, pH 7.3;10 mL per 400 mL of original culture volume) and frozen. After thawing, cell lysis was completed by the addition of lysozyme to a final concentration of 0.01mg/mL and Triton X-100 at 0.1% v/v and incubated at RT for 20 min followed by the addition of 0.02 mg/mL DNase I and 10 mM $MgCl_2$ until the viscosity of the solution was reduced followed by 2 min of pulsed sonication on ice. Insoluble fusion protein was then recovered from the total cell lysate by centrifugation (10 min, 12000 g) and purified by re-suspension in wash buffer (50 mM Tris-HCl, 10 mM EDTA, 0.5% Triton X-100, pH 8; 2.5 mL per 400 mL of original culture volume) and recovering by centrifugation (10 min, 12000 g), with this step repeated again with wash buffer and then a further two times with dH_2O.

Purified petide-protein inclusion bodies were solubilised with 6 mL of 85% formic acid and peptide released from the fusion by addition of 0.2 g cyanogen bromide, incubated in the dark at RT for 16-24 h. After incubation the formic acid solution was diluted with 20 mL of dH_2O and lyophilised. Soluble peptides were then separated from the insoluble KSI stirring overnight in PBS (25 mM Na_2HPO_4, 100 mM NaCl; 2.5 mL per 400 mL original culture volume) the pH corrected to 7.5 and recovered by centrifugation. Peptide was then separated and purified from the contaminating His-tag using a Waters 600/486 series HPLC with a preparative Vidac C18 reverse phase protein and peptide column using an elution gradient of HPLC grade water and 70% acetonitrile / 30% water containing 0.05% and 0.045% trifluoroacetic acid (TFA) respectively. Peptide containing fractions were collected when the absorbance of the flow at 220 nm reached

0.1 AU and stopped when the absorbance returned to 0.2 AU to minimise the risk of sample contamination. Collected fractions were then lyophilised to recover the peptide.

Detailed NMR data acquisition, processing and analysis for structure determination

NMR experiments were carried out at 10 °C on a Varian UnityINOVA spectrometer operating at 14.1 Tesla (^{1}H resonance frequency of 600 MHz) with a 5 mm HCN z-pulse field gradient probe using standard biological NMR experiments[2] with modifications as described. All chemical shift referencing in the ^{1}H dimension was completed using the relationship between temperature and ^1H_2O resonance (10 °C / 4.945 ppm)[3] and referencing in the ^{15}N and ^{13}C dimensions using a non-standard VNMR macro on the spectrometer that uses ^{1}H referencing based on the HDO resonance and adjusted to ^{13}C and ^{15}N using gamma ratios.[3] With the exception of the 30% d_3-TFE 2D TOCSY and NOESY experiments, all spectra were collected with WATERGATE solvent suppression to reduce intensity from the water signal. Solvent suppression for the 30% d_3-TFE 2D TOCSY and NOESY experiments was achieved with a presaturation pulse of 1 s, as hydroxyl protons from the TFE are in fast exchange with the water as a result of the proton signal intensities attributed to d_3-TFE. All NMR data were processed using NMRpipe[4] on Linux PCs.

^{15}N-^{1}H HSQC experiments of all peptides were run with 2048 data points (8000 Hz) in the direct F2 dimension and 128 points (2000 Hz) in the F1 dimension with 16 transients. 2D TOCSY experiments were collected with 2048/512 data points (8000 Hz in both dimensions) over 16 transients with a mixing time of 80 ms. 2D NOESY experiments were collected with 2048/512 data points (8000 Hz in both dimensions) with a mixing time of 250 ms over 16 transients in accordance with previously published data.[5] As the peptides analysed were ^{15}N enriched, the TOCSY and NOESY experiments were modified to contain ^{15}N decoupling. In addition signal overlap and data complexity were reduced using 3D TOCSY-HSQC and NOESY-HSQC experiments. These were run with 2048 points (8000 Hz) in the ^{1}H F3 dimension, 128 points (8000 Hz) in the ^{1}H F2 dimension and 24 points (2000 Hz) in the ^{15}N F1 dimension. NOESY experiments used a mixing time of 250 ms, and TOCSY experiments an 80 ms mixing time over 16 transients.

Once processed, all NMR spectra were assigned using the software package CCPN Analysis.[6] A theoretical chemical structure for the tri-peptide Arg-Thr-HSL was used to predict the following proton chemical shifts for homoserine lactone using the programs HNMR predictor and ChemSketch from the ACD/labs V9.0 (Advanced Chemistry Development, Inc. Toronto, Canada): H^{α} 4.51; $H^{\beta a/\beta b}$ 2.20/2.84 and $H^{\gamma a/\gamma b}$ 4.44/4.69 ppm. Chemical shift perturbation maps for backbone resonances from ^{15}N HSQCs were completed using the following equation: $\Delta\delta=\sqrt{[(\delta N/5)^2+(\delta H)^2]}$, where $\Delta\delta$, δH and δN are the difference in the average chemical shift, the proton chemical shift and the nitrogen chemical shift respectively.

SUPPLEMENTARY RESULTS

Structure determination of peptides in 30%(v/v) trifluoroethanol

TOCSY and NOESY datasets were used for side chain assignments and through-space structural information for the peptides in the presence of 30% TFE. Once assigned, NOESY cross peaks were collated as restraint data sets for structure calculation and refinement using CNS. Ensembles of the 50 lowest energy structures calculated for each peptide are shown in Figure S2 where the ensembles are superimposed on their

respective helical regions. Each structure in the ensemble was water-refined using YASARA Structure and Figure 1 illustrates the structure closely resembling the mean from each peptide ensemble as backbone ribbon diagrams with the side chains of the RGDLxxL motif labelled.

All 4 peptides exhibit the necessary turn-helix motif for αvβ6 recognition with the RGD residues found N-terminal to an α-helix of varying length: from residue Leu10-Ala18 for FMDV2, from Gln11-Ala19 for DBD1 and Leu10-Gln15 for DBD2. The ribbon structure of LAP2 shows that, as is the case with the FMDV based peptides, the leucine/isolecuines of the binding motif appear on the same face of helix. The defined helix limits shown with key NOE contacts and restraints in the structure schematic of Figure 2 and structural statistics for the ensembles are shown in Table S2.

The limits of helices analysed by dihedral angle analysis confirmed most-favoured and additionally allowed regions in PROCHECK-NMR as being attributed to the structural portion of the peptide. Generously allowed and disallowed regions are found for random coil unstructured regions of the peptide and are greatest in both LAP2 and DBD2 peptides; both peptides with the shortest length of helix. Interestingly, FMDV2 has comparably low generously allowed and disallowed regions to DBD1, despite not being pinned in a cyclic conformation. This suggests FMDV2 adopts a significant structural arrangement beyond the helix in TFE and this is also confirmed by the detection of medium range NOE's from Pro4 to Arg6.

Assignment of NMR spectra in the absence and presence of trifluoroethanol

The assignment of each peptide ^{15}N-^{1}H HSQC was completed using standard sequential assignment methods with both 2D and 3D TOCSY and NOESY datasets. The assigned ^{15}N-^{1}H HSQCs of each peptide in the presence and absence of TFE are shown in the supplementary material (Figure S1) and the full resonance assignments of each peptide are also listed in the supplementary material (Table S1).

The assignment of proton resonances for FMDV2 in phosphate buffer and 30% d_3-TFE was completed to 96 and 97% respectively. For DBD1 total proton assignment was 83% in phosphate buffer and 86% in TFE. For DBD2 the total proton assignment was 96% in phosphate and 92% in TFE. For LAP2 the total proton assignment was 90% in phosphate and 94% in TFE. Lower percentage assignment in phosphate buffer reflects the collapse of resonances due to the random coil state.

The ^{15}N HSQCs collected for the non-disulphide bonded peptides in phosphate buffer FMDV2 and LAP2 appear as a typically unfolded peptide with the majority of the backbone peaks between 8.0 and 8.5 ppm. On addition of 30% d_3-TFE, peak dispersion increases supporting these peptide having adopted a structured conformation. The ^{15}N HSQCs of the DBD1 and DBD2 (disulphide bonded peptides) in phosphate buffer, exhibit dispersion that is not characteristic of an unfolded peptide. However the positions of the HSQC peaks do significantly shift on addition of 30% d_3-TFE and the inspection of NOESY data for DBD1 and DBD2 in phosphate buffer supports that no alpha helical secondary structure exists suggesting the observed dispersion is created due to cyclisation and the compact topology of the peptides in its oxidized form.

Figure S1

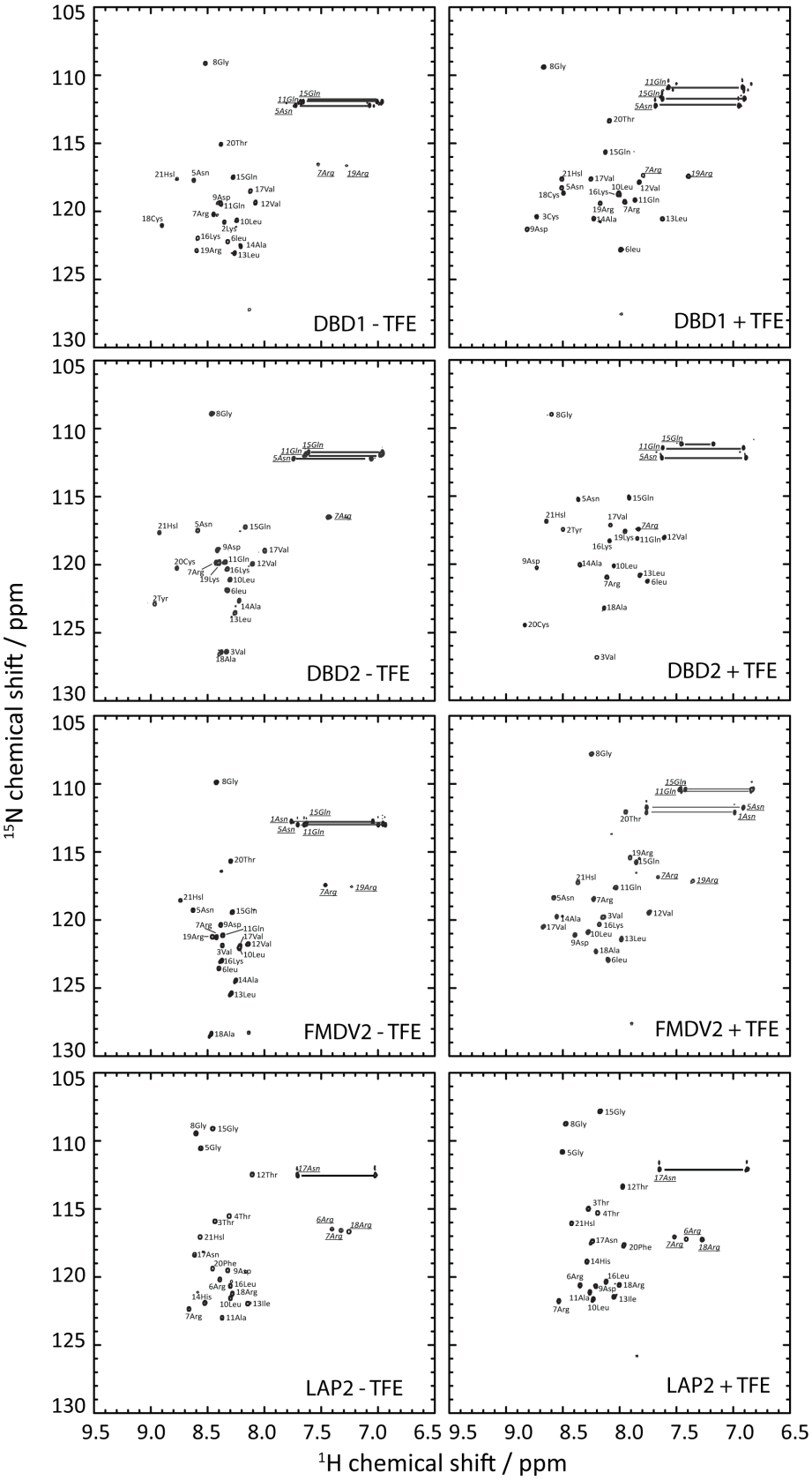

Figure S1. *^{15}N HSQC spectra for peptides +/- TFE (with assignment labels)*

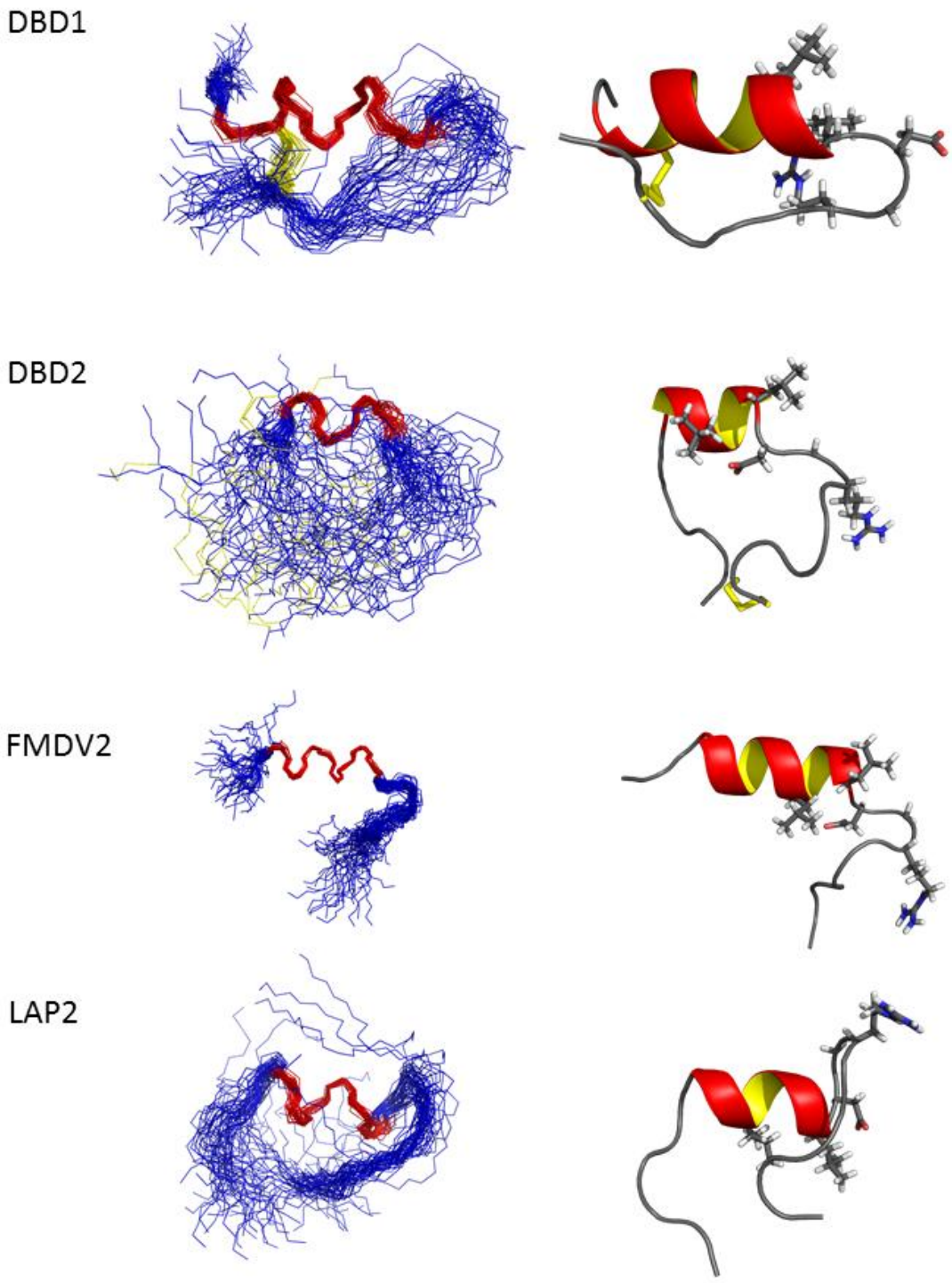

Figure S2. *Structural ensembles with RMSD fits using the helix region*

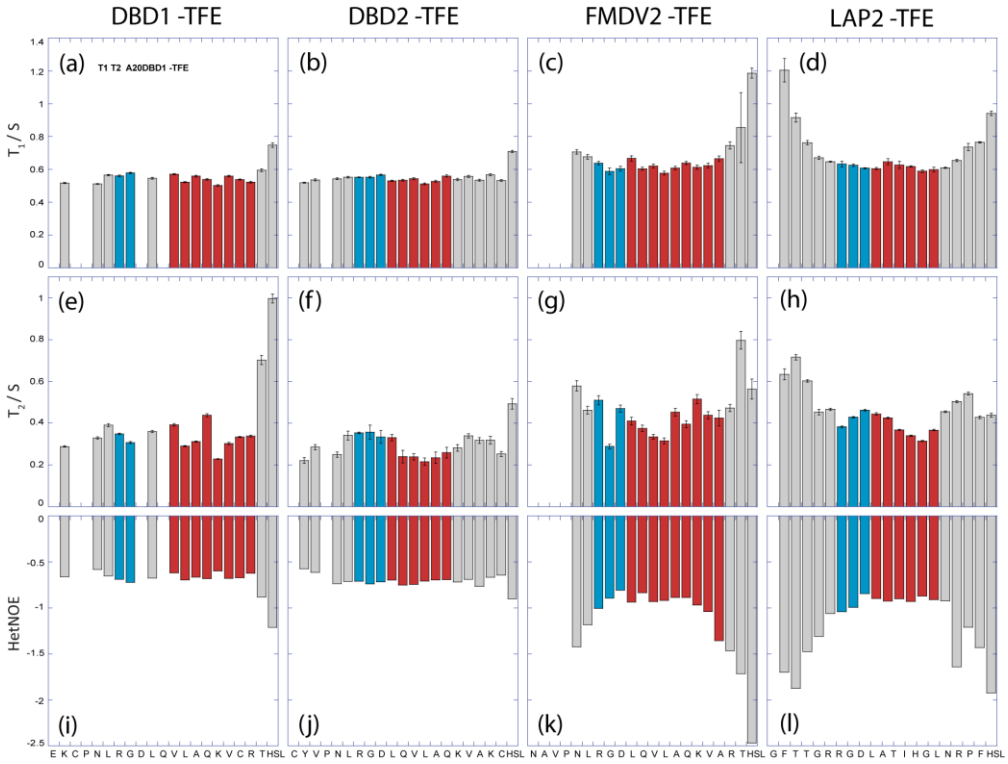

Figure S3. *^{15}N T_1, T_2 and hetNOE Relaxation data in the absence of TFE.* Data reporting within TFE defined structure regions from Figures 1 and 2 are coloured blue for RGD-turn and red for the helix region for each peptide.

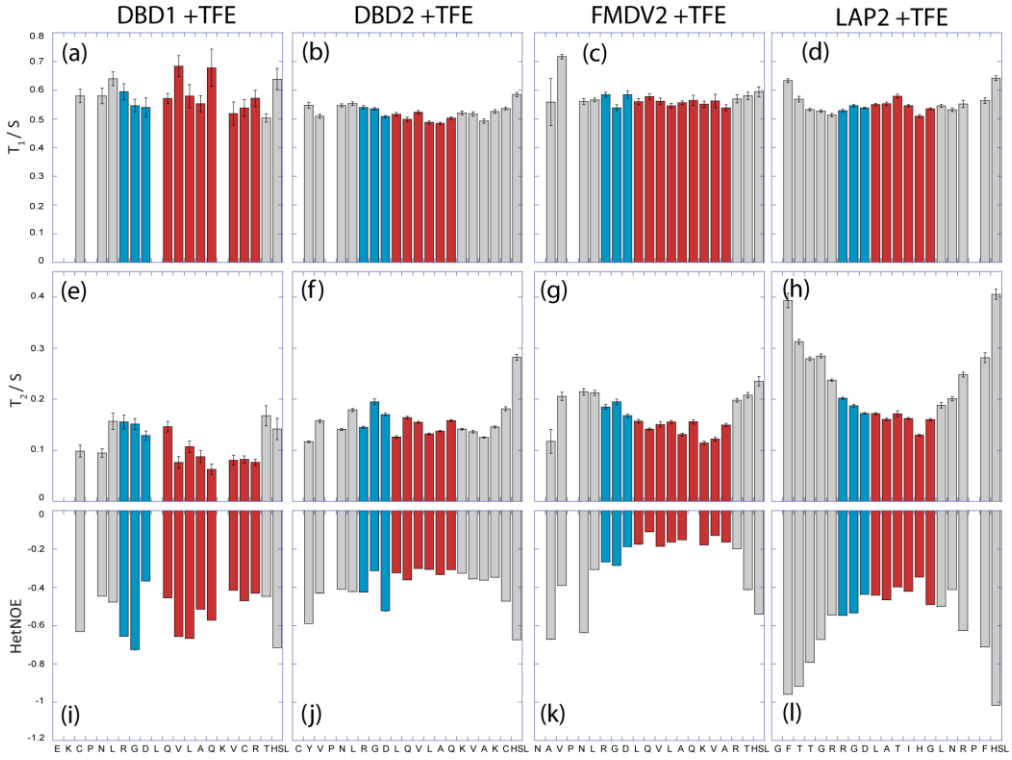

Figure S4. *^{15}N T_1, T_2 and hetNOE relaxation data in the presence of 30%(v/v) TFE* Data reporting within TFE defined structure regions from Figures 1 and 2 are coloured blue for RGD-turn and red for the helix region for each peptide.

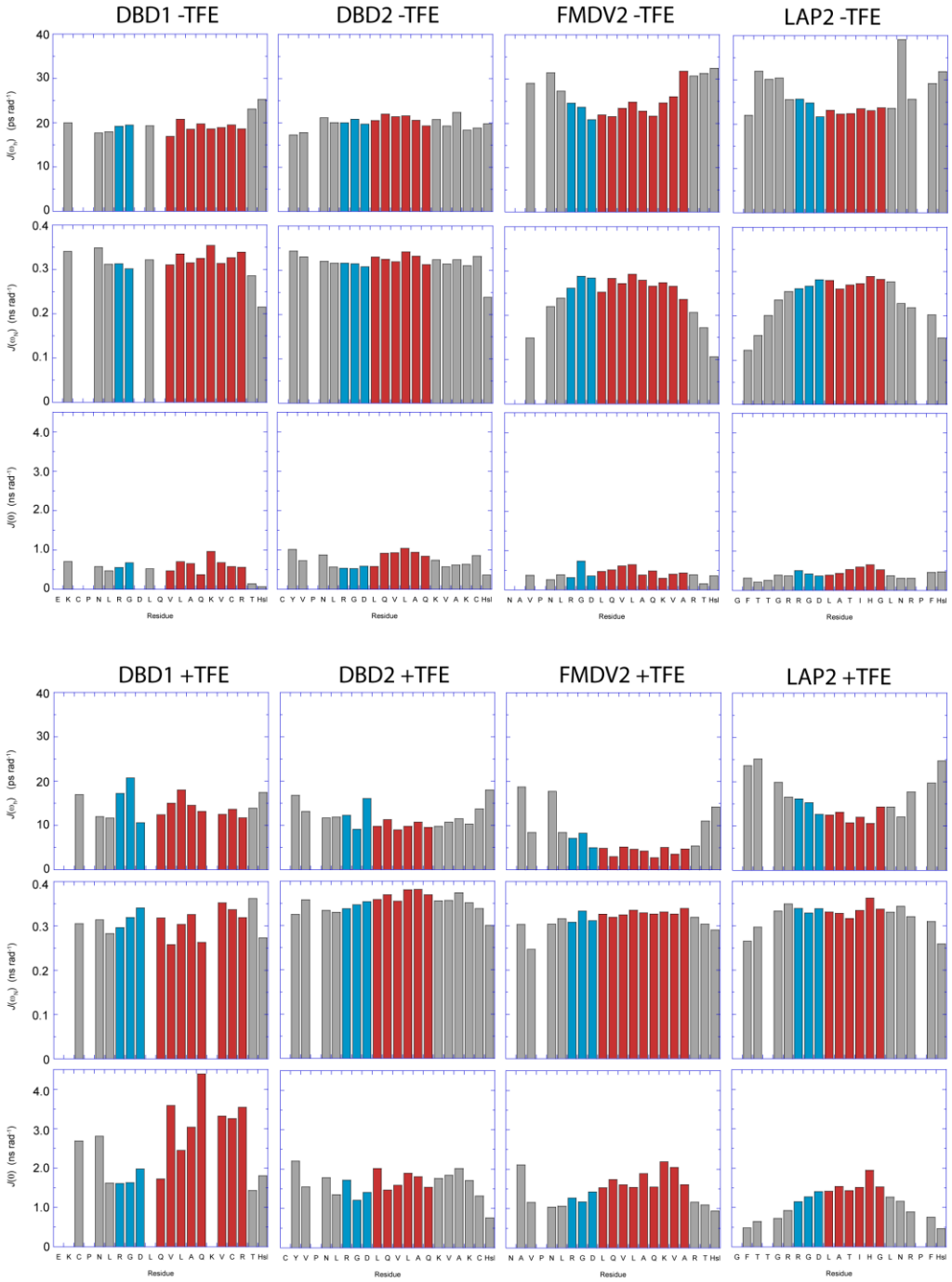

Figure S5. *^{15}N reduced spectral density data in the absence and presence of 30%(v/v) TFE* Data reporting within TFE defined structure regions from Figures 1 and 2 are shaded grey for RGD-turn and black for the helix region for each peptide.

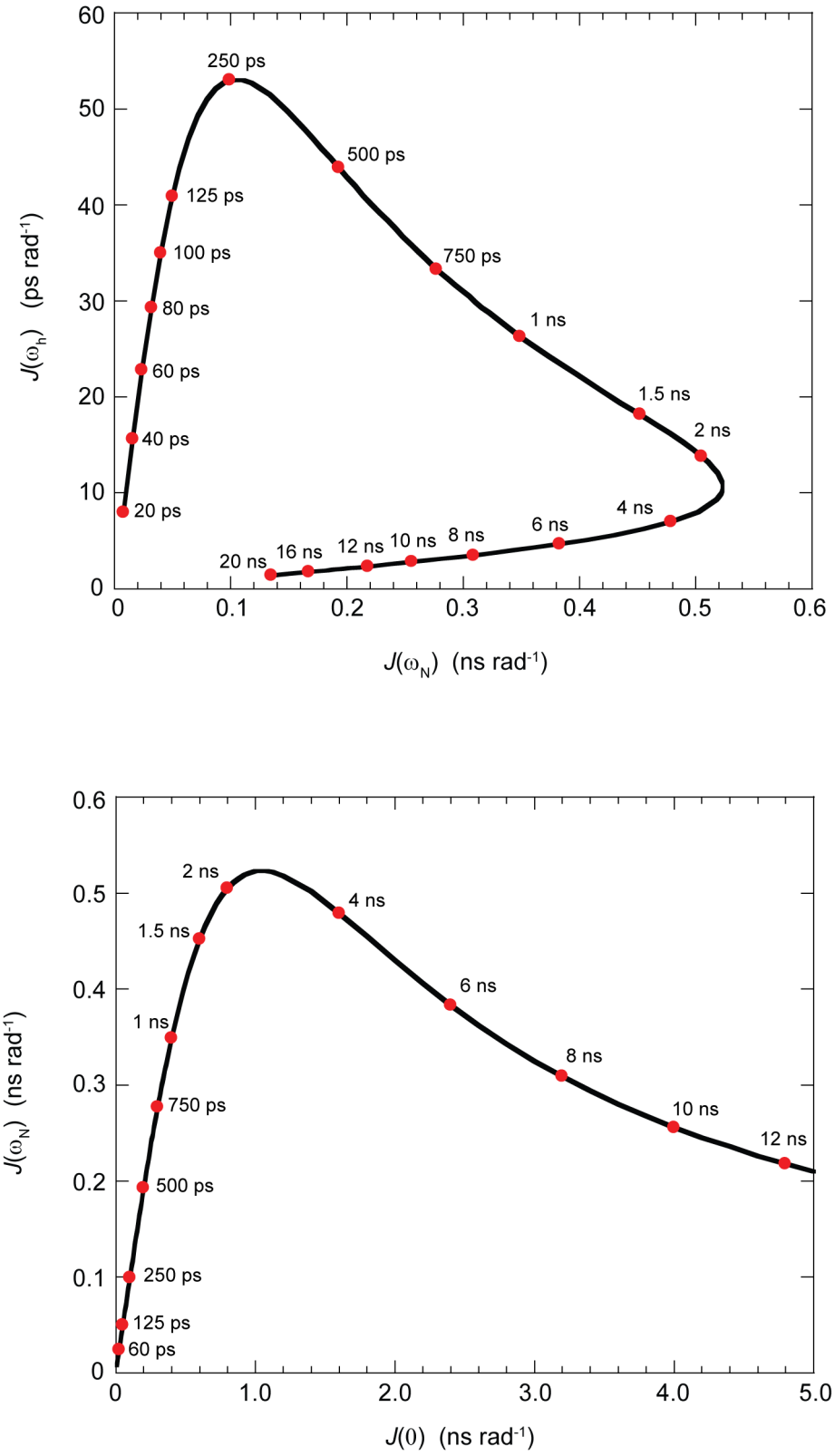

Figure S6. *Spectral density plots showing timescales of motion*

FACS Data

A

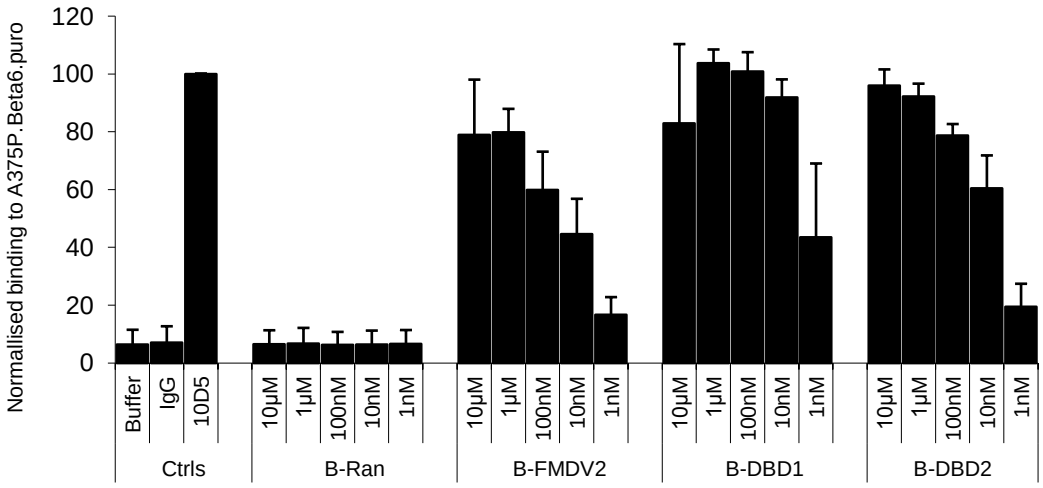

B

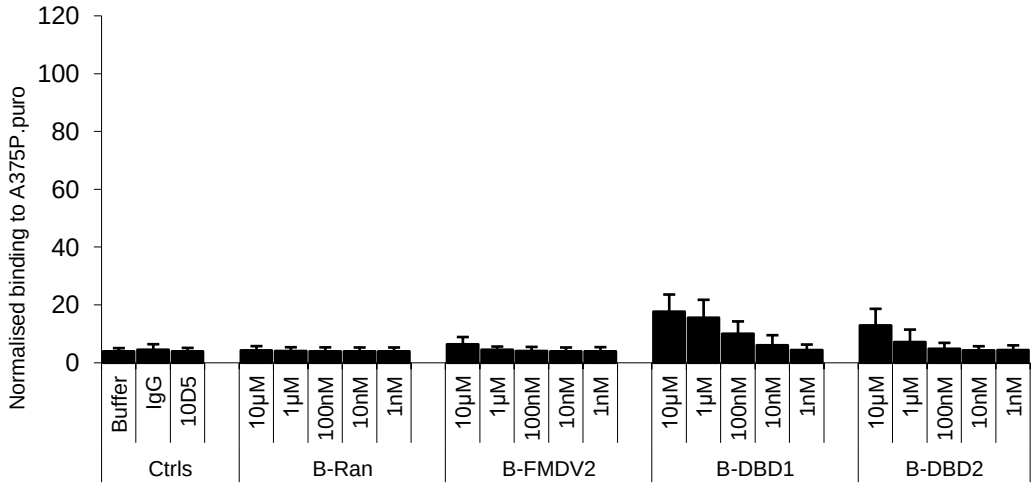

Figure S7: Binding of biotinylated peptides to A375P.puro and A375P.Beta6.puro by flow cytometry.

Binding of biotinylated peptides to cell lines A375P.Beta6.puro (A) and A375P.puro (B) by flow cytometry. Binding is shown normalised to the signal given by anti-alphaVbeta6 antibody 10D5 on A375P.Beta6.puro. Binding of scrambled control peptide B-Ran (Biotin-eykCKLVGALQPDNVLQRCRTK) is shown for comparison. Data represent mean and standard deviation of 3 or 4 experiments.

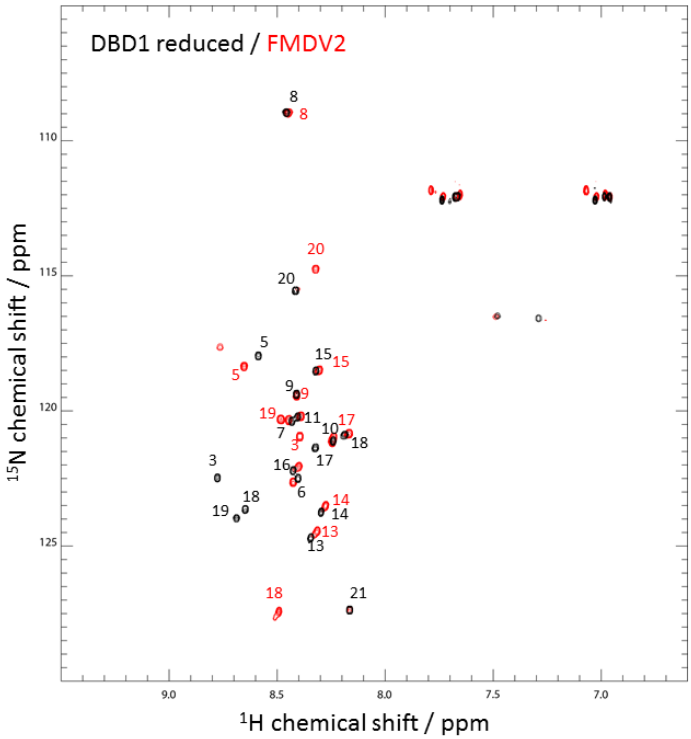

Figure S2. ^{15}N HSQC showing similarities of DBD1 (reduced) and FMDV2.

^{15}NH assignment residue numbers are shown on each peak.

Figure S8. *^{15}N HSQC overlay of FMDV2 and reduced DBD1 peptide showing peptide similarities*

^{15}N HSQC data for DBD1 in the presence of the chemical reducing agent dithiothreitol (DTT) collapses the spectrum of this peptide with the spectrum showing remarkable similarity to FMDV2, with the exception of amino acids directly flanking both cysteine residues. This result is exactly what would be expected as DBD1 is a cyclized peptide based on the FMDV2 sequence and supports the primary difference between these peptides being the cyclisation process.

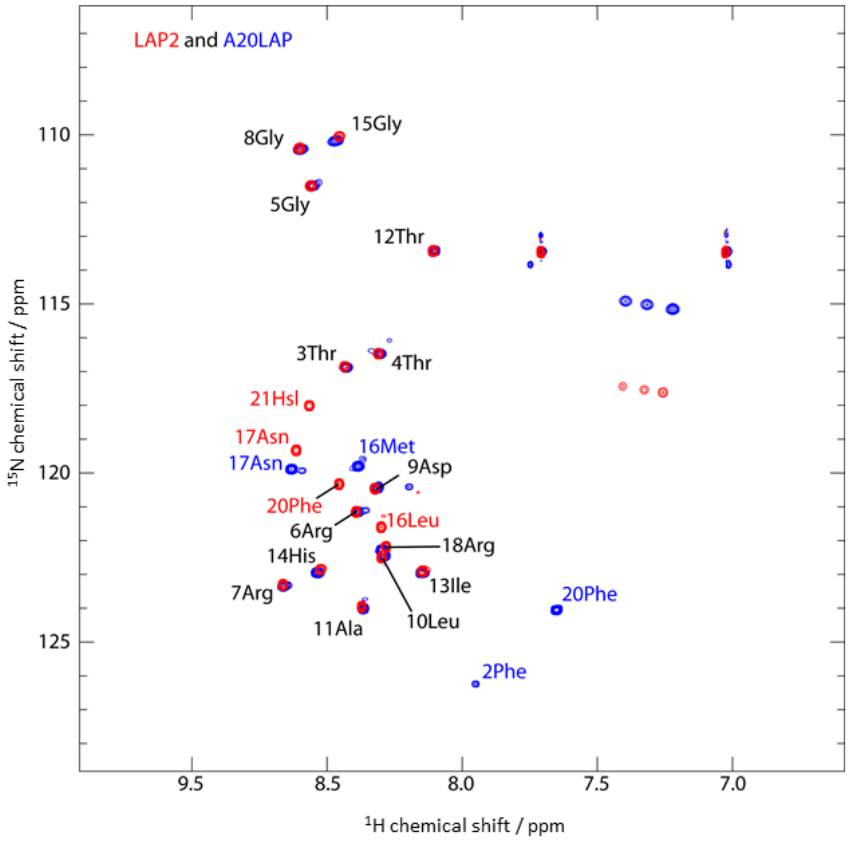

Figure S9. ^{15}N HSQC overlay of 1mM LAP2 (red) and 0.2 mM A20LAP (blue) in PBS, pH 6.5, 10°C. Common assignments in black and specific peptide assignments in the appropriate colour.

Only residues to show significant chemical shift changes in LAP2 from A20LAP are 16L/16M (M16L mutation) and 17 Asn.

Differences observed for 20F are due to the presence of 21Hsl (homoserine lactone) from CNBr cleaving during peptide purification from the KSI fusion partner.

The three Arg sidechain peaks at δ_{1H} 7.2-7.4 are shifted between LAP2 and A20LAP because they are folded into the spectrum and different ^{15}N carrier and window sizes were used.

^{15}N A20LAP was made by expressing the peptide sequence as a fusion: GST-(GluC cleavage site)-peptide using a pGEX-6P-2 vector in *E.coli* BL21(DE3)pLysS. The fusion protein was isolated using glutathione sepharose and the peptide was GFTTGRRGDLATIHGMNRPF separated from the fusion using GluC peptidase. Final purification of the peptide from GST was achieved using RP-HPLC. Peptide yields from the GST-peptide fusion approach were extremely low compared to the insoluble KSI-fusion method and hence was not adopted for peptide production for NMR relaxation analysis in this study. GST-peptide quantities were insufficient for structural and dynamic analysis.

Table S1. *All peptide ^{15}N and ^{1}H NMR assignments in the absence and presence of 30%(v/v) TFE*

S-1.1 Chemical shifts (ppm) of ^{15}N-DBD1 in PBS

Residue	N	H^N	H^α	Others
1Glu				
2Lys	120.785	8.350	4.303	$H^{\beta2/\beta3}$ 1.856 1.904; $H^{\gamma1/\gamma2}$ 1.452; $H^{\delta1/\delta2}$ 1.716; $H^{\varepsilon2}$ 3.046
3Cys				
4Pro			4.461	$H^{\beta2/\beta3}$ 1.972, 2.325; H^{γ} 2.068; $H^{\delta1/\delta2}$ 3.786, 3.849
5Asn	117.687	8.622	4.712	$H^{\beta2/\beta3}$ 2.796, 2.880; $H^{\delta21/\delta22}$ 7.076, 7.723; $N^{\delta2}$ 112.217
6Leu	122.229	8.321	4.438	$H^{\beta2/\beta3}$ 1.696; H^{γ} 1.631; $H^{\delta1/\delta2}$ 0.902, 0.969
7Arg	120.235	8.445	4.381	$H^{\beta2/\beta3}$ 1.841, 1.950; $H^{\gamma1/\gamma2}$ 1.688; $H^{\delta1/\delta2}$ 3.271; H^{ε} 7.471; N^{ε} 115.791
8Gly	109.151	8.517	3.942	
9Asp	119.439	8.388	4.612	$H^{\beta2/\beta3}$ 2.693, 2.765
10Leu	120.634	8.243	4.340	$H^{\beta2/\beta3}$ 1.753; H^{γ} 1.638; $H^{\delta1/\delta2}$ 0.903, 0.978
11Gln	119.416	8.385	4.321	$H^{\beta2/\beta3}$ 2.066, 2.146; $H^{\gamma1/\gamma2}$ 2.405; $H^{\varepsilon21/\varepsilon22}$ 6.964, 7.682; $N^{\varepsilon2}$ 111.927
12Val	119.341	8.078	4.086	H^{β} 2.150; $H^{\gamma1/\gamma2}$ 0.989
13Leu	123.098	8.260	4.328	$H^{\beta2/\beta3}$ 1.726; H^{γ} 1.636; $H^{\delta1/\delta2}$ 0.913, 0.982
14Ala	122.829	8.207	4.306	H^{β} 1.447
15Gln	117.523	8.275	4.306	$H^{\beta2/\beta3}$ 2.059, 2.179; $H^{\gamma1/\gamma2}$ 2.437; $H^{\varepsilon21/\varepsilon22}$ 7.007, 7.655; $N^{\varepsilon2}$ 111.911
16Lys	121.947	8.587	4.758	
17Val	118.487	8.124	4.176	H^{β} 2.127; $H^{\gamma1/\gamma2}$ 0.984
18Cys	121.045	8.899	4.786	$H^{\beta2/\beta3}$ 2.965, 3.282
19Arg	122.899	8.597	4.511	$H^{\beta2/\beta3}$ 1.842, 1.932; $H^{\gamma1/\gamma2}$ 1.687; H^{ε} 7.307; N^{ε} 115.904
20Thr	115.075	8.383	4.380	H^{β} 4.257; $H^{\gamma1}$ 1.270
21Hsl	117.642	8.768	4.726	$H^{\beta2/\beta3}$ 2.405, 2.267; $H^{\gamma1/\gamma2}$ 4.434, 4.587

S-1.2 Chemical shifts (ppm) of ^{15}N-DBD1 in 30% d_3-TFE

Residue	N	H^N	H^α	Others
1Glu				
2Lys				
3Cys	120.414	8.727		$H^{\beta2/\beta3}$ 3.110, 3.269
4Pro			4.489	$H^{\beta2/\beta3}$ 1.949, 2.337; H^{γ} 2.050; $H^{\delta1/\delta2}$ 3.755, 3.858
5Asn	118.521	8.504	4.768	$H^{\beta2/\beta3}$ 2.788, 2.897; $H^{\delta21/\delta22}$ 6.949, 7.682; $N^{\delta2}$ 112.253
6Leu	122.808	7.989	4.533	$H^{\beta1/\beta2}$ 1.651; H^{γ} 1.562; $H^{\delta1/\delta2}$ 0.937, 0.967
7Arg	119.307	7.952	4.524	$H^{\beta2/\beta3}$ 1.864, 2.016; $H^{\gamma1/\gamma2}$ 1.756; $H^{\delta1/\delta2}$ 3.289; H^{ε} 7.795; N^{ε} 117.355
8Gly	109.382	8.665	3.923	
9Asp	121.319	8.812	4.560	$H^{\beta2/\beta3}$ 2.737, 2.813
10Leu	118.696	8.007	4.434	$H^{\beta2/\beta3}$ 1.885; H^{γ} 1.775; $H^{\delta1/\delta2}$ 0.949, 1.047
11Gln	119.167	7.866	4.157	$H^{\beta2/\beta3}$ 2.172, 2.234; $H^{\gamma1/\gamma2}$ 2.495; $H^{\varepsilon21/\varepsilon22}$ 6.919, 7.568; $N^{\varepsilon2}$ 110.905
12Val	117.858	7.825	3.891	H^{β} 2.245; $H^{\gamma1/\gamma2}$ 1.054, 1.133
13Leu	120.538	7.623	4.258	$H^{\beta2/\beta3}$ 1.798; H^{γ} 1.731; $H^{\delta1/\delta2}$ 0.930, 0.970
14Ala	120.534	8.225	4.149	H^{β} 1.572
15Gln	115.650	8.124	4.192	$H^{\beta2/\beta3}$ 2.238, 2.306; $H^{\gamma1/\gamma2}$ 2.574; $H^{\varepsilon21/\varepsilon22}$ 6.904, 7.624; $N^{\varepsilon2}$ 111.726
16Lys	118.694	8.005	4.253	$H^{\beta2/\beta3}$ 1.894, 2.069; $H^{\gamma1/\gamma2}$ 1.526; $H^{\delta1/\delta2}$ 1.634; $H^{\varepsilon2}$ 2.404
17Val	117.607	8.250	4.008	H^{β} 2.244; $H^{\gamma1/\gamma2}$ 1.012, 1.077
18Cys	118.585	8.492	4.583	$H^{\beta2/\beta3}$ 3.409, 3.351
19Arg	119.400	8.168	4.465	$H^{\beta2/\beta3}$ 3.351, 3.409; $H^{\gamma1/\gamma2}$ 1.763, 2.052; $H^{\delta1/\delta2}$ 3.294; H^{ε} 7.393; N^{ε} 117.406
20Thr	113.297	8.089	4.451	H^{β} 4.356; $H^{\gamma1}$ 1.346
21Hsl	117.621	8.509	4.771	$H^{\beta2/\beta3}$ 2.491, 2.705; $H^{\gamma1/\gamma2}$ 4.451, 4.613

S-1.3 Chemical shifts (ppm) of ^{15}N-DBD2 in PBS

Residue	N	H^N	H^α	Others
1Cys			4.467	
2Thr	122.873	8.964	4.829	
3Val	126.402	8.331	4.309	$H^{\beta2/\beta3}$ 0.910, 0.936
4Pro			4.331	
5Asn	117.493	8.586	4.685	$H^{\beta2/\beta3}$ 2.867, 2.900; $H^{\delta21/\delta22}$ 7.059, 7.745; $N^{\delta2}$ 112.240
6Leu	121.900	8.322	4.399	$H^{\beta2/\beta3}$ 1.698; H^{γ} 1.642; $H^{\delta1/\delta2}$ 0.909, 0.939
7Arg	119.848	8.422	4.368	$H^{\beta2/\beta3}$ 1.838, 1.945; $H^{\gamma1/\gamma2}$ 1.653, 1.697; $H^{\delta1/\delta2}$ 3.255; H^{ε} 7.437; N^{ε} 116.504
8Gly	108.922	8.463	3.937	
9Asp	118.940	8.411	4.666	$H^{\beta2/\beta3}$ 2.785, 2.845
10Leu	121.113	8.301	4.327	$H^{\beta2/\beta3}$ 1.703; H^{γ} 1.623; $H^{\delta1/\delta2}$ 0.903, 0.957
11Gln	119.848	8.341	4.314	$H^{\beta2/\beta3}$ 2.036, 2.122; $H^{\gamma1/\gamma2}$ 2.378; $H^{\varepsilon21/\varepsilon22}$ 6.978, 7.686; $N^{\varepsilon2}$ 119.848
12Val	119.968	8.104	4.048	H^{β} 2.113; $H^{\gamma1/\gamma2}$ 0.948, 0.977
13Leu	123.543	8.257	4.305	$H^{\beta2/\beta3}$ 1.667, 1.692; H^{γ} 1.605; $H^{\delta1/\delta2}$ 0.888, 0.945
14Ala	122.666	8.219	4.265	H^{β} 1.427
15Gln	117.263	8.166	4.286	$H^{\beta2/\beta3}$ 2.034, 2.123; $H^{\gamma1/\gamma2}$ 2.398; $H^{\varepsilon21/\varepsilon22}$ 6.962, 7.611; $N^{\varepsilon2}$ 111.739
16Lys	120.330	8.326	4.312	$H^{\beta2/\beta3}$ 1.830, 1.894; $H^{\gamma1/\gamma2}$ 1.430
17Val	118.962	7.995	4.168	H^{β} 2.121; $H^{\gamma1/\gamma2}$ 0.965, 0.992
18Ala	126.412	8.376	4.363	H^{β} 1.432
19Lys	119.845	8.399	4.308	$H^{\beta2/\beta3}$ 1.803, 1.850; $H^{\gamma1/\gamma2}$ 1.460; $H^{\delta1/\delta2}$ 1.725
20Cys	120.243	8.768	4.706	$H^{\beta2/\beta3}$ 3.005, 3.292
21Hsl	117.655	8.923	4.723	$H^{\gamma1/\gamma2}$ 4.430, 4.588

S-1.4 Chemical shifts (ppm) of ^{15}N-DBD2 in 30% d_3-TFE

Residue	N	H^N	H^α	Others
1Cys				
2Tyr	117.428	8.497	4.756	$H^{\beta2/\beta3}$ 3.198, 3.338 H^δ 7.121; H^ε 6.856
3Val	126.834	8.198	4.376	$H^{\beta2/\beta3}$ 0.898, 0.963
4Pro			4.305	$H^{\beta2/\beta3}$ 1.949, 2.346; H^γ 2.023; $H^{\delta1/\delta2}$ 3.630
5Asn	115.235	8.364	4.616	$H^{\beta2/\beta3}$ 2.919; $H^{\delta21/\delta22}$ 6.887, 7.630; $N^{\delta2}$ 112.164
6Leu	121.268	7.757	4.519	$H^{\beta2/\beta3}$ 1.584, 1.635; H^γ 1.537; $H^{\delta1/\delta2}$ 0.906
7Arg	120.961	8.113	4.510	$H^{\beta2/\beta3}$ 1.878, 2.026; $H^{\gamma1/\gamma2}$ 1.771; $H^{\delta1/\delta2}$ 3.295; H^ε 7.834; N^ε 117.404
8Gly	108.998	8.599	3.930	
9Asp	120.298	8.729	4.574	$H^{\beta2/\beta3}$ 2.826, 2.889
10Leu	120.117	8.051	4.316	$H^{\beta2/\beta3}$ 1.806, 1.896; H^γ 1.689; $H^{\delta1/\delta2}$ 0.950, 1.039
11Gln	118.095	7.843	4.033	$H^{\beta2/\beta3}$ 2.079, 2.281; $H^{\gamma1/\gamma2}$ 2.467; $H^{\varepsilon21/\varepsilon22}$ 7.175, 7.459; $N^{\varepsilon2}$ 111.155
12Val	118.056	7.607	3.828	H^β 2.266; $H^{\gamma a/\gamma b}$ 1.027, 1.114
13Leu	120.815	7.824	4.153	$H^{\beta2/\beta3}$ 1.802; H^γ 1.731; $H^{\delta1/\delta2}$ 0.938, 0.974
14Ala	120.028	8.351	4.087	H^β 1.503
15Gln	115.110	7.917	4.167	$H^{\beta2/\beta3}$ 2.281, 2.597; $H^{\gamma1/\gamma2}$ 2.667; $H^{\varepsilon21/\varepsilon22}$ 6.909, 7.623; $N^{\varepsilon2}$ 111.488
16Lys	118.301	8.089	4.283	
17Val	117.148	8.081	4.085	H^β 2.252; $H^{\gamma1/\gamma2}$ 1.013, 1.048
18Ala	123.202	8.137	4.334	H^β 1.522
19Lys	117.554	7.955	4.371	$H^{\beta2/\beta3}$ 1.783, 1.958; $H^{\gamma1/\gamma2}$ 1.515; $H^{\delta1/\delta2}$ 1.551 $H^{\varepsilon2}$ 3.101
20Cys	124.485	8.835	4.764	$H^{\beta2/\beta3}$ 2.940, 3.086
21Hsl	116.875	8.644	4.728	$H^{\beta2/\beta3}$ 2.454, 2.688; $H^{\gamma1/\gamma2}$ 4.440, 4.611

S-1.5 Chemical shifts (ppm) of ^{15}N-A20fmdv2 in PBS

Residue	N	H^N	H^α	Others
1Asn			4.712	$H^{\beta2/\beta3}$ 2.866, 2.930; $H^{\delta21/\delta22}$ 7.046, 7.766; $N^{\delta2}$ 112.751
2Ala	118.516	8.719	4.404	
3Val	121.860	8.373	4.403	H^{β} 2.105; $H^{\gamma1/\gamma2}$ 0.934, 1.055
4Pro				
5Asn	119.274	8.631	4.688	$H^{\beta2/\beta3}$ 2.813, 2.871; $H^{\delta21/\delta22}$ 7.000, 7.708; $N^{\delta2}$ 112.940
6Leu	123.657	8.402	4.363	$H^{\beta2/\beta3}$ 1.696; H^{γ} 1.594; $H^{\delta1/\delta2}$ 0.892, 0.935
7Arg	121.294	8.427	4.313	$H^{\beta2/\beta3}$ 1.807, 1.931; $H^{\gamma1/\gamma2}$ 1.654; $H^{\delta1/\delta2}$ 3.240; H^{ε} 7.471; N^{ε} 117.442
8Gly	109.896	8.429	3.957	
9Asp	120.457	8.392	4.584	$H^{\beta2/\beta3}$ 2.754
10Leu	121.952	8.224	4.303	$H^{\beta2/\beta3}$ 1.706; H^{γ} 1.655; $H^{\delta1/\delta2}$ 0.947, 0996
11Gln	121.142	8.374	4.289	$H^{\beta2/\beta3}$ 2.032, 2.101; $H^{\gamma1/\gamma2}$ 2.375; $H^{\varepsilon21/\varepsilon22}$ 6.937, 7.651; $N^{\varepsilon2}$ 112.990
12Val	121.838	8.146	4.024	H^{β} 2.088; $H^{\gamma1/\gamma2}$ 0.921, 1.014
13Leu	125.407	8.299	4.340	$H^{\beta2/\beta3}$ 1.682; H^{γ} 1.600; $H^{\delta1/\delta2}$ 0.895, 0.959
14Ala	124.435	8.256	4.282	H^{β} 1.407
15Gln	119.394	8.284	4.284	$H^{\beta2/\beta3}$ 1.997, 2.123; $H^{\gamma1/\gamma2}$ 2.416; $H^{\varepsilon21/\varepsilon22}$ 6.958, 7.631; $N^{\varepsilon2}$ 112.926
16Lys	123.025	8.379	4.289	$H^{\beta2/\beta3}$ 2.061, 2.365; $H^{\gamma1/\gamma2}$ 1.445; $H^{\delta1/\delta2}$ 1.819; $H^{\varepsilon2}$ 3.032
17Val	121.959	8.221	4.091	H^{β} 2.084; $H^{\gamma1/\gamma2}$ 0.918, 0.989
18Ala	128.359	8.467	4.406	
19Arg	121.233	8.462	4.401	$H^{\beta2/\beta3}$ 1.804, 1.919; $H^{\gamma1/\gamma2}$ 1.653; $H^{\delta1/\delta2}$ 3.237; H^{ε} 7.243; N^{ε} 117.559
20Thr	115.687	8.300	4.394	H^{β} 4.306; $H^{\gamma1}$ 1.244
21Hsl	118.587	8.745	4.735	$H^{\beta2/\beta3}$ 2.376, 2.646; $H^{\gamma1/\gamma2}$ 4.411, 4.588

S-1.6 Chemical shifts (ppm) of ^{15}NA20fmdv2 in 30% d_3-TFE

Residue	N	H^N	H^α	Others
1Asn			4.157	$H^{\beta2/\beta3}$ 2.889; $H^{\delta21/\delta22}$ 6.990, 7.770; $N^{\delta2}$ 112.237
2Ala	118.563	8.259	4.424	H^{β} 1.733
3Val	119.926	8.149	4.481	H^{β} 2.193; $H^{\gamma1/\gamma2}$ 1.043, 1.087
4Pro			4.445	$H^{\beta2/\beta3}$ 1.961, 2.358; $H^{\gamma1/\gamma2}$ 2.094; $H^{\delta1/\delta2}$ 3.765, 3.920
5Asn	118.515	8.584	4.807	$H^{\beta2/\beta3}$ 2.829, 3.020; $H^{\delta21/\delta22}$ 6.914, 7.770; $N^{\delta2}$ 111.852
6Leu	123.091	8.106	4.377	$H^{\beta2/\beta3}$ 1.717; H^{γ} 1.712; $H^{\delta1/\delta2}$ 0.953, 1.006;
7Arg	118.592	8.230	4.246	$H^{\beta2/\beta3}$ 1.932, 2.000; $H^{\gamma1/\gamma2}$ 1.715, 1.795; $H^{\delta1/\delta2}$ 3.285; H^{ε} 7.670; N^{ε} 116.996
8Gly	107.946	8.254	3.972	
9Asp	121.233	8.398	4.555	$H^{\beta2/\beta3}$ 2.798
10Leu	121.021	8.280	4.243	$H^{\beta2/\beta3}$ 1.842, 1.899; H^{γ} 1.678; $H^{\delta1/\delta2}$ 0.949, 0.994
11Gln	117.754	8.038	4.118	$H^{\beta2/\beta3}$ 2.455, 2.580; $H^{\gamma1/\gamma2}$ 2.278; $H^{\varepsilon21/\varepsilon22}$ 6.838, 7.472; $N^{\varepsilon2}$ 110.506
12Val	119.600	7.743	3.787	H^{β} 2.311; $H^{\gamma1/\gamma2}$ 1.042, 1.163
13Leu	121.571	7.983	4.137	$H^{\beta2/\beta3}$ 1.889, 1.935; H^{γ} 1.754; $H^{\delta1/\delta2}$ 0.950, 0.980
14Ala	119.823	8.556	4.048	H^{β} 1.567
15Gln	115.890	7.855	4.141	$H^{\beta2/\beta3}$ 2.500, 2.676; $H^{\gamma1/\gamma2}$ 2.303;$H^{\varepsilon21/\varepsilon22}$ 6.844, 7.424; $N^{\varepsilon2}$ 110.531
16Lys	120.450	8.181	4.150	$H^{\beta2/\beta3}$ 1.729, 2.111; $H^{\gamma1/\gamma2}$ 1.690; $H^{\delta1/\delta2}$ 1.490; $H^{\varepsilon2}$ 2.997
17Val	120.618	8.672	3.766	H^{β} 2.226; $H^{\gamma1/\gamma2}$ 0.997, 1.098
18Ala	122.454	8.212	4.223	H^{β} 1.584
19Arg	115.562	7.908	4.358	$H^{\beta2/\beta3}$ 1.981, 2.085; $H^{\gamma1/\gamma2}$ 1.804, 1.911; $H^{\delta1/\delta2}$ 3.280; H^{ε} 7.363; N^{ε} 117.237
20Thr	112.172	7.952	4.423	H^{β} 4.375; $H^{\gamma1}$ 1.357
21Hsl	117.398	8.370	4.762	$H^{\beta2/\beta3}$ 2.487, 2.689; $H^{\gamma1/\gamma2}$ 4.445, 4.593

S-1.7 Chemical shifts (ppm) of ^{15}N-A20lap2 in PBS

Residue	N	H^N	H^α	Others
1Gly				
2Phe				
3Thr	115.931	8.435	4.475	H^β 4.255; $H^{\gamma1}$ 1.231
4Thr	115.525	8.308	4.377	H^β 4.299; $H^{\gamma1}$ 1.282
5Gly	110.541	8.561	4.022	
6Arg	120.226	8.394	4.398	$H^{\beta2/\beta3}$ 1.791, 1.888; H^γ 1.655; $H^{\delta1/\delta2}$ 3.230; H^ε 7.321; N^ε 116.594
7Arg	122.369	8.662	4.331	$H^{\beta2/\beta3}$ 1.842, 1.917; $H^{\gamma1/\gamma2}$ 1.693; $H^{\delta1/\delta2}$ 3.240; H^ε 7.405; N^ε 116.482
8Gly	109.453	8.603	3.976	
9Asp	119.548	8.324	4.637	$H^{\beta2/\beta3}$ 2.701, 2.755
10Leu	121.550	8.298	4.330	$H^{\beta2/\beta3}$ 1.707; H^γ 1.627; $H^{\delta1/\delta2}$ 0.913, 0.971
11Ala	123.034	8.374	4.359	H^β 1.450
12Thr	112.477	8.108	4.319	H^β 4.221; $H^{\gamma1}$ 1.196
13Ile	121.950	8.146	4.153	H^β 1.862; $H^{\gamma12/\gamma13}$ 1.174, 1.417
14His	121.910	8.524	4.730	$H^{\beta2/\beta3}$ 3.153, 3.266
15Gly	109.081	8.454	3.987	
16Leu	120.661	8.298	4.375	$H^{\beta2/\beta3}$ 1.700; H^γ 1.625; $H^{\delta1/\delta2}$ 0.913, 0.971
17Asn	118.394	8.614	4.715	$H^{\beta2/\beta3}$ 2.773, 2.852; $H^{\delta21/\delta22}$ 7.027, 7.711; $N^{\delta2}$ 118.394
18Arg	121.252	8.282	4.652	$H^{\beta2/\beta3}$ 1.738, 1.850; $H^{\gamma1/\gamma2}$ 1.668; $H^{\delta1/\delta2}$ 3.237; H^ε 7.258; N^ε 116.687
19Pro			4.425	$H^{\beta2/\beta3}$ 1.848, 2.267; $H^{\gamma1/\gamma2}$ 2.022; $H^{\delta1/\delta2}$ 3.651, 3.785
20Phe	119.376	8.456	4.601	$H^{\beta2/\beta3}$ 3.146
21Hsl	117.115	8.567	4.357	$H^{\beta2/\beta3}$ 2.264, 2.529; $H^{\gamma1/\gamma2}$ 4.383

S-1.8 Chemical shifts (ppm) of ^{15}N-A20lap2 in 30% d_3-TFE

Residue	N	H^N	H^α	Others
1Gly				
2Phe	125.796	7.848	4.306	
3Thr	115.001	8.269	4.518	H^β 4.351; $H^{\gamma1}$ 1.271
4Thr	115.291	8.192	4.415	H^β 4.371; $H^{\gamma1}$ 1.338
5Gly	110.877	8.501	4.068	
6Arg	120.594	8.343	4.474	$H^{\beta2/\beta3}$ 1.861, 1.984; H^γ 1.704; $H^{\delta1/\delta2}$ 3.278; H^ε 7.413; N^ε 117.157
7Arg	121.777	8.530	4.329	$H^{\beta2/\beta3}$ 1.916, 1.980; $H^{\gamma1/\gamma2}$ 1.725, 1.801; $H^{\delta1/\delta2}$ 3.286; H^ε 7.517; N^ε 117.091
8Gly	108.712	8.208	4.008	
9Asp	120.643	8.208	4.673	$H^{\beta2/\beta3}$ 2.849
10Leu	121.667	8.229	4.239	$H^{\beta2/\beta3}$ 1.788, 1.849; H^γ 1.672; $H^{\delta1/\delta2}$ 0.964, 1.023
11Ala	121.127	8.259	4.259	H^β 1.557
12Thr	113.384	7.972	4.424	H^β 4.243; $H^{\gamma1}$ 1.308
13Ile	121.427	8.047	3.987	H^β 1.944; $H^{\gamma12/\gamma13}$ 1.240, 1.594; $H^{\gamma2}$ 0.893; $H^{\delta1}$ 0.855
14His	118.893	8.286	4.622	$H^{\beta2/\beta3}$ 3.189, 3.358; $H^{\delta1/\delta2}$ 0.953, 0.993
15Gly	107.843	8.172	4.042	
16Leu	120.329	8.115	4.418	$H^{\beta2/\beta3}$ 1.800; H^γ 1.685; $H^{\delta1/\delta2}$ 0.953, 0.993
17Asn	117.392	8.240	4.787	$H^{\beta2/\beta3}$ 2.819, 2.885; $H^{\delta21/\delta22}$ 6.878, 7.647; $N^{\delta2}$ 112.070
18Arg	120.590	8.002	4.687	$H^{\beta2/\beta3}$ 1.789, 1.861; $H^{\gamma1/\gamma2}$ 1.709; $H^{\delta1/\delta2}$ 3.262; H^ε 7.273; N^ε 117.174
19Pro			4.451	$H^{\beta2/\beta3}$ 1.886, 2.261; $H^{\gamma1/\gamma2}$ 2.039; $H^{\delta1/\delta2}$ 3.659, 3.793
20Phe	117.673	7.959	4.680	$H^{\beta2/\beta3}$ 3.203; H^ζ 7.338
21Hsl	116.047	8.420	4.587	$H^{\beta2/\beta3}$ 2.368, 2.568; $H^{\gamma1/\gamma2}$ 4.409, 4.531

		DBD1	DBD2	FMDV2	LAP2
NOE					
	Total	117	60	150	144
	Intra-residue	6	5	17	12
	i, i+1	88	43	96	101
	i, i >1	23	12	37	31
Hydrogen bonds		7	2	6	5
Dihedral angles		9	6	9	6
NOE violations >0.2 Å		0	0	0	0
Energy (kJ mol^{-1})		-760.2	-394.6	-958.9	-510.9
RMSD					
	Backbone (N, CA, C) (Å)				
	All	1.70	2.60	1.67	2.25
	Helix	0.37	0.39	0.23	0.31
	Heavy atoms				
	All	3.09	4.21	2.57	3.36
	Helix	2.59	3.69	2.01	2.92
Ramachandran plot regions (%)					
	Most favoured	71.2	56.1	61.1	58.0
	Additionally allowed	22.7	33.5	33.3	25.9
	Generously allowed	3.6	6.4	2.8	12.4
	Disallowed	2.5	4.0	2.8	3.7

Table S2. *Structural Statistics for the 50 ensemble structures of each peptide in 30% (v/v) TFE..*

References

1. Wagstaff, J. L., Howard, M. J. & Williamson, R. A. (2010). Production of recombinant isotopically labelled peptide by fusion to an insoluble partner protein: generation of integrin alphavbeta6 binding peptides for NMR. *Mol Biosyst* **6**, 2380-5.
2. Cavanagh, J., Fairbrother, W., Palmer, A., Rance, M. & Skelton, N. (2007). *Protein NMR Spectroscopy: Principles and Practice*. 2nd edit, Academic Press.
3. Wishart, D. S. & Sykes, B. D. (1994). Chemical shifts as a tool for structure determination. *Methods in Enzymology* **239**, 363-369.
4. Delaglio, F., Grzesiek, S., Vuister, G. W., Zhu, G., Pfeifer, J. & Bax, A. (1995). NMRPipe: a multidimensional spectral processing system based on UNIX pipes. *J Biomol NMR* **6**, 277-93.
5. DiCara, D., Rapisarda, C., Sutcliffe, J. L., Violette, S. M., Weinreb, P. H., Hart, I. R., Howard, M. J. & Marshall, J. F. (2007). Structure-function analysis of Arg-Gly-Asp helix motifs in alpha v beta 6 integrin ligands. *Journal of Biological Chemistry* **282**, 9657-65.
6. Vranken, W. F., Boucher, W., Stevens, T. J., Fogh, R. H., Pajon, A., Llinas, M., Ulrich, E. L., Markley, J. L., Ionides, J. & Laue, E. D. (2005). The CCPN data model for NMR spectroscopy: development of a software pipeline. *Proteins* **59**, 687-96.